Springer

KSME

Journal of Mechanical Science and Technology 24 (11) (2010) 2233~2239
www.springerlink.com/content/1738-494x
DOI 10.1007/s12206-010-0802-9

An inscribed surface model for the elastic properties of armchair carbon nanotube †

Sheng Lu[1], Chongdu Cho[1,*], Kyu-won (Ken) Choi[2], Wonjun Choi[1], Sangkyo Lee[1] and Na Wang[1]

[1]*Department of Mechanical Engineering, Inha University, Inchon, 402-751, Korea*
[2]*Department of Electrical and Computer Engineering, Illinois Institute of Technology, Chicago, IL60616, USA*

(Manuscript Received August 6, 2009; Revised March 23, 2010; Accepted July 18, 2010)

Abstract

With special physical structure and novel properties, single walled carbon nanotubes (SWCNTs) have attracted much attention in science and engineering. In order to develop a direct link between continuum analysis and atomistic simulation to investigate the mechanical properties of CNTs more effectively, an innovatory methodology to construct continuum model from the inner (inscribed surface) to the outer (covalent bond) is developed. Present study begins from studying Cauchy-Born rule. The differential geometry concept of inscription and the mean value theorem are adopted to modify the Cauchy-Born rule, and then this modified Cauchy-Born rule can build a hyper-elastic inscribed surface constitutive model. Resorting to using Tersoff-Brenner potential, the current theory to armchair CNTs is applied to evaluate the mechanical properties. The results are validated by the comparison with previously reported studies.

Keywords: Carbon nanotube; Constitutive model; Interatomic potential; Curvature; Deformation gradient

1. Introduction

Since macroscopic amounts of multi-walled carbon nanotubes (MWCNTs) were synthesized [1], CNTs have attracted much attention in science and engineering, owing to their many unique and novel properties: low density, specific stiffness, excellent electrical and thermal conductivities. In order to have a fundamental understanding of mechanical properties of CNTs and accommodate those excellent properties in mechanical applications, a series of experiments have been performed [2-5]. At the same time, numerous theoretical and numerical ways have been proposed to understand and predict the mechanical properties of CNTs.

Based on atomistic simulations such as molecular dynamics [6-8], tight-binding methods [9] and first-principle calculations [10, 11], a series of values of mechanical properties of CNTs are given and agreed qualitatively with experimental studies, but such methods quickly become computationally extremely demanding as the number of atoms increases. In other words, there exists a rigorous limitation in the atomistic simulation by its time and length scales.

Based on classical continuum mechanics, a series of models such as cylindrical shell model [12], beam model [13] and structural mechanics [14] have been proposed. From a computational point of view, those continuum models are much more efficient, but the linkage between atomistic and continuum descriptions of material properties is still not well established.

In order to develop a direct link between continuum analysis and atomistic simulation to investigate the mechanical properties of CNTs more effectively, the concept of atomistic continuum has been gradually developed. Tadmor et al. [15, 16] first proposed a quasi-continuum model to link atomistic simulation with continuum analysis for solid materials. Gao et al. [17] developed a virtual internal bond model to construct the constitutive model of solids from atomic level. Zhang et al. [18-20] incorporated the interatomic potential directly into a constitutive model based on the modified Cauchy-Born rule in application to CNTs. Jiang et al. [21] took the effect of tube radius into account based on the work of Zhang et al. [19]. Arroyo and Belytschko [22, 23] proposed the exponential Cauchy-Born rule by introducing the exponential map to extend the standard Cauchy-Born rule to describe the deformation of CNTs much more accurately. Guo et al. [24] studied the mechanical properties of CNTs by using the higher order terms of the deformation gradient. Lu et al. [25] proposed a type of modified Cauchy-Born rule to investigate the strain energy of armchair CNTs.

The outline of present paper is as follows: Tersoff-Brenner interatomic potential for carbon is summarized and applied to hexagonal atomic structure to acquire an equilibrium bond length in Section 2. Cauchy-Born rule and its limitations are introduced in Section 3. Section 4 shows the modified Cauchy-Born rule is extended into inscribed surface. Section 5 makes a discussion in detail about the nonlinear deformation

† This paper was recommended for publication in revised form by Associate Editor Maenghyo Cho

*Corresponding author. Tel.: +82 32 860 7321, Fax: +82 32 873 9069
E-mail address: cdcho@inha.ac.kr

gradient in the process of deforming. Subsequently, in Section 6 one hyper-elastic inscribed surface constitutive model is developed. With the use of the proposed constitutive model, the mechanical properties of armchair CNTs are also predicted. Finally, Section 7 gives discussions of results and some concluding remarks.

2. The interatomic potential for carbon

Tersoff-Brenner interatomic potential for carbon [26, 27], which is widely used in the researches for CNTs, is introduced as follows:

$$V(r_{ij}) = V_R(r_{ij}) - B_{ij}V_A(r_{ij}) \,. \tag{1}$$

In Eq. (1), i and j represent the respective carbon atoms at the ends of one covalent bond. r_{ij} is the distance between i and j. The repulsive interaction V_R and attractive interaction V_A between two carbon atoms are given by:

$$\begin{aligned} V_R(r) &= f_c(r)\frac{D_e}{S-1}e^{-\sqrt{2S}\beta(r-r_e)} \\ V_A(r) &= f_c(r)\frac{D_e S}{S-1}e^{-\sqrt{2/S}\beta(r-r_e)} \end{aligned} \tag{2}$$

where the parameters D_e = 6.000eV, S =1.22, β =21nm^{-1} and r_e =0.1390 nm in Eq. (2) are determined from the known physical properties of carbon, graphite and diamond. The multi-body coupling term B_{ij} represents the coupling between the bond ij and the local environment of atom i, which is given by:

$$B_{ij} = \left[1 + \sum_{K(\neq i,j)} G(\theta_{ijk}) f_c(r_{ik})\right]^{-\delta} , \tag{3}$$

where δ = 0.50000, r_{ik} is the distance between atom i and its local environmental atom k and θ_{ijk} is the angle between the bond ij and ik ($k \neq i, j$, see Fig. 1).

The smooth cutoff function f_c both in Eq. (2) and Eq. (3), which restricts the pair potential to nearest neighbors with r_1 =0.17 nm and r_2 =0.20 nm, is given by

$$f_c(r) = \begin{cases} 1 & r < r_1 \\ \frac{1}{2}\{1+\cos[\frac{\pi(r-r_1)}{(r_2-r_1)}]\} & r_1 \le r \le r_2 \\ 0 & r > r_2 \end{cases} . \tag{4}$$

The function $G(\theta)$ in Eq. (3) is given by

$$G(\theta) = a_0\left[1 + \frac{c_0^2}{d_0^2} - \frac{c_0^2}{d_0^2 + (1+\cos\theta)^2}\right] , \tag{5}$$

with a_0 = 0.00020813, c_0 =330 and d_0 = 3.5.

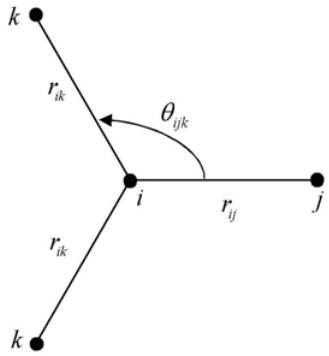

Fig. 1. The carbon atoms i, j and k in the hexagonal atomic structure.

With this set of parameters, the potential function is applied into the hexagonal atomic structure as shown in Fig. 1. The equilibrium bond length can be determined by

$$\partial V / \partial r_{ij} = 0 \,. \tag{6}$$

Eq. (6) gives the equilibrium bond length a_{cc} = 0.145068nm, which is in good agreement with that of graphite (0.144nm).

3. The standard Cauchy-Born rule and its limitations

Cauchy-Born rule [28] plays an important role in the atomistic continuum mechanics, which is the fundamental kinematics assumption that establishes a connection between the deformation of an atomic system and that of a continuum. It is widely accepted as the form of

$$\mathbf{a} = \mathbf{F} \cdot \mathbf{A} \,, \tag{7}$$

where $\mathbf{F}$ denotes a two-point deformation gradient tensor, $\mathbf{A}$ and $\mathbf{a}$ denote one lattice vector in the respective undeformed and deformed crystals. In the absence of diffusion, phase transition, slip, lattice defect and other non-homogeneities, Eq. (7) is good at describing the deformation of bulk material.

Noticeably, there are two limitations to solid materials in the application of the standard Cauchy-Born rule: one is that the solid material must be simple Bravais lattice, the other is that the material must be a type of bulk material, or equivalently, space-filling material. Unfortunately, neither of two limitations is satisfied by the structure of CNTs.

The deformation gradient $\mathbf{F}$ only can describe the variation of infinitesimal material vector in its tangent space. For the vectors of a finite length in space-filling material, the body and its tangent vector are always undistinguishable, so it is allowed to use tangent space to describe material space. For curved crystalline films, especially for one-atom-thick layer, which is different from space-filling crystal, the tangent space of infinitesimal material vectors can not coincide with the finite length lattice vector. In other words, the deformation gradient $\mathbf{F}$ maps the tangent spaces of the surface, but the

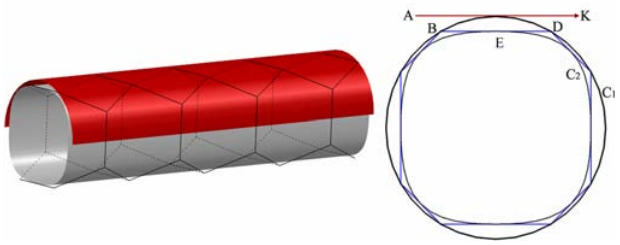

Fig. 2. The relationships between the atomic surface and inscribed surface of CNT structures. The inner configuration is inscribed surface, and the outer configuration is atomic surface.

lattice vectors should be regarded as chords of the surface, so the deformation gradient $\mathbf{F}$ can not give an accurate description of relationship between the undeformed and the deformed lattice vectors. This issue restricts the applications of the standard Cauchy-Born rule in the curved crystalline films, such as CNTs, especially for CNTs with large curvature.

4. The modified Cauchy-Born rule based on the inscribed surface

Due to the position of atoms, generally SWCNT is viewed as the cylindrical surface as the outer red surface as shown in Fig. 2. This surface, called as atomic surface, is denoted by C_1. If the standard Cauchy-Born rule is applied to the atomic surface C_1, it means that the deformation of the bond BD is described by tangent behavior along the direction of AK. So errors will be inevitably introduced. However, the chord BD is in coincidence with the tangent of the inscribed surface C_2 at the point E; in other words, the bond BD is the tangent of the inscribed surface C_2 at the point E. That is to say, the variations of the bonds (the chords of the atomic surface C_1) can be investigated by the deformation gradient of the inscribed surface C_2 at each tangent point.

How to link this inscribed surface to Cauchy-Born rule? From the continuum mechanics point of view, the linear transformation between the two line segments is given by

$$\mathrm{d}\mathbf{x} = \mathbf{F}\,\mathrm{d}\mathbf{X} \ , \tag{8}$$

where $\mathrm{d}\mathbf{x}$ and $\mathrm{d}\mathbf{X}$ denote one infinitesimal line segment joining two material particles in the deformed and the undeformed configurations, respectively; $\mathbf{F}$ is the deformation gradient tensor. Integrating Eq. (8) by taking the finite length of the lattice vectors $\mathbf{a}$ and $\mathbf{A}$ into account, Eq. (8) can be written as:

$$\int_{\mathbf{x}}^{\mathbf{x}+\mathbf{a}} \mathrm{d}\mathbf{x} = \int_{\mathbf{X}}^{\mathbf{X}+\mathbf{A}} \mathbf{F}\,\mathrm{d}\mathbf{X}. \tag{9}$$

The corresponding deformed lattice vector $\mathbf{a}$ can be expressed as

$$\mathbf{a} = \int_{\mathbf{X}}^{\mathbf{X}+\mathbf{A}} \mathbf{F}\,\mathrm{d}\mathbf{X}. \tag{10}$$

If the deformation gradient tensor $\mathbf{F}$ is smooth enough on the closed interval $[\mathbf{X}, \mathbf{X}+\mathbf{A}]$, it is natural to introduce mean value theorem in calculus. To be brief, there exists a certain point $\mathbf{X}_\alpha \in [\mathbf{X}, \mathbf{X}+\mathbf{A}]$ such that

$$\mathbf{a} = \mathbf{F}(\mathbf{X}_\alpha)\,\mathbf{A}. \tag{11}$$

Comparing Eq. (11) with Eq. (7), the main difference is from deformation gradient tensor. For space-filling crystals, the body coincides with its tangent particularly well, so all the deformation gradients of every infinitesimal line segment on the interval $[\mathbf{X}, \mathbf{X}+\mathbf{A}]$ are the same and can be used to express the deformation gradient of whole lattice vector $\mathbf{A}$; however, for curved crystalline films, every infinitesimal line segment on interval $[\mathbf{X}, \mathbf{X}+\mathbf{A}]$ has its own deformation gradient.

Bravais multi-lattices as graphite sheet can be considered as a collections of interpenetrating simple Bravais lattices. So, the inner shift vector $\boldsymbol{\lambda}$ between two sub-lattices should be taken into consideration since the inner shift can occur without disobeying Cauchy-Born rule [29]. Then, the bond vector can be expressed as:

$$\mathbf{a} = \mathbf{F}(\mathbf{X}_\alpha, \boldsymbol{\lambda}) \cdot (\mathbf{A} + \boldsymbol{\lambda}) \ . \tag{12}$$

The inner shift $\boldsymbol{\lambda}$ can lead the deformation gradient to have a self-adjustment to make the structure reach the most stable state in any time of deforming. For explanations in detail, see Section 5.

Now, inscribed surface introduced in the above can be combined with the modified Cauchy-Born rule. Eq. (12) can be used in CNTs by their inscribed surface. In Eq. (12), $\mathbf{A}$ and $\mathbf{a}$ denote one lattice vector in the undeformed and the deformed crystals, respectively; $\mathbf{F}(\mathbf{X}_\alpha, \boldsymbol{\lambda})$ denotes the deformation gradient of a tangent point on the inscribed surface. So the method of using the deformation gradient of the tangent point on inscribed surface to describe the lattice vector of a single layer crystalline film is developed.

5. Nonlinear deformation gradient

Firstly, a triangle in the graphite sheet as shown in Fig. 3 can be introduced as a representative cell **I**. All dashed lines in Fig. 3 are symmetry axes, so any two adjacent representative cells possess axial symmetry. So both graphite sheet and CNT consist of representative cells.

Fig. 4 shows the process of rolling up a graphite sheet into an armchair CNT. A planar graphite sheet of equilibrium energy state is defined as the undeformed configuration. At this state, it is simple to find that inscribed surface coincides with atomic surface substantially. With the mapping of the rolling up graphite sheet into a hollow cylinder, atomic surface and inscribed surface of the graphite sheets have their own configurations, respectively. As shown in Fig. 4, the outer one (in red color) is the deformed atomic surface, and the inner one (in gray color) is the deformed inscribed surface. Obviously,

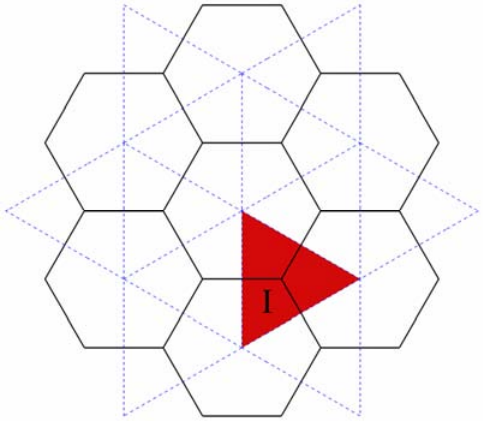

Fig. 3. Representative cell corresponding to a carbon atom.

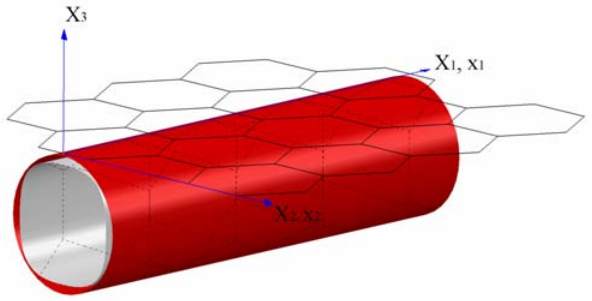

Fig. 4. Illustration of rolling up a graphite sheet into an armchair CNT (2, 2).

the two surfaces abide by two different mappings.

Fig. 5 shows the cross section of an armchair CNT in the whole process of rolling up deformation. In the undeformed state, atomic surface coincides completely with inscribed surface. The black width lines *PQ* and *QR* along the axis $\mathbf{X}_2$ denote the representative cell *A* and *B*, respectively. In the deformed state, three dashed lines from the outer to the inner (in red, black and blue colors) denote the configurations of atomic surface, C-C bonds and inscribed surface without considering the inner shift vector $\boldsymbol{\lambda}$, respectively. Following the same logic, three solid lines from the outer to the inner show the configurations of atomic surface, C-C bonds and inscribed surface with incorporating the inner shift vector $\boldsymbol{\lambda}$, respectively. With considering the inner shift, obvious changes in C-C bonds can be observed from the deformed part of Fig. 5. However, by comparing with the inner dashed curve (inscribed surface without considering the inner shift), the inner solid curve *pqr* (inscribed surface with considering the inner shift) has obvious changes in its shape, which becomes much flatter than before. From the view of energy, the curve with small curvature will be much steadier than with large curvature, so it is not difficult to say that the inner shift let the deformation gradient itself have an adjustment to make energy surface become steady. This standpoint will be proved from theory as follows.

The curve *pq* in Fig. 5, which is a cubic curve in the deformed coordinates (x_1, x_2, x_3), can be determined by positions and tangents of two end points. Combined with the undeformed coordinates (X_1, X_2), the mapping of the inscribed surface *pq* can be expressed as:

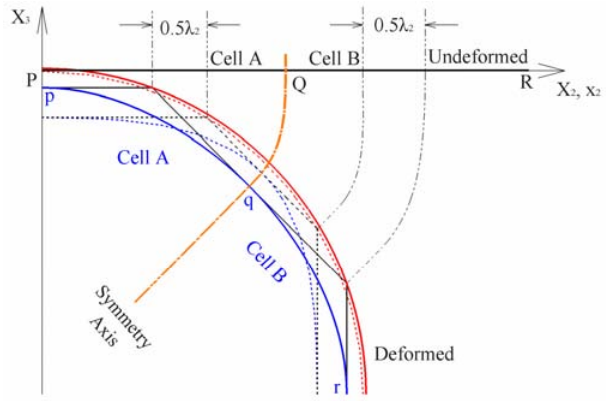

Fig. 5. The mapping of rolling up deformation for an armchair CNT.

$$\begin{aligned} x_1 &= X_1, \\ x_2 &= eX_2, \\ x_3 &= aX_2^{\,3} + bX_2^{\,2} + cX_2 + d \end{aligned} \quad , \tag{13}$$

where (x_1, x_2, x_3) are the point coordinates in current configuration, (X_1, X_2) are the point coordinates in the undeformed configuration. The coefficients *a, b, c, d, e*, which are functions of nanotube chiral (*n, m*) and the inner shift $\boldsymbol{\lambda}$, can be determined from geometric relations. Then the deformation gradient can be obtained as:

$$\mathbf{F}(\mathbf{X}_\alpha, \boldsymbol{\lambda}) = \begin{bmatrix} 1 & 0 & 0 \\ 0 & e & 0 \\ 0 & 3aX_\alpha^2 + 2bX_\alpha + c & 0 \end{bmatrix}. \tag{14}$$

Therefore, the deformation gradient for this rolling mapping not only has relationships with determination of the tangent point $\mathbf{X}_\alpha$, but also depends on the inner shift $\boldsymbol{\lambda}$. The inner shift $\boldsymbol{\lambda}$ is determined by minimizing the strain energy, so determination of the deformation gradient must be after step of minimizing the strain energy. That is to say, when the deformation gradient is determined, the corresponding structure must have minimum strain energy already at that state. In other words, the deformation gradient will have a self-adjustment by inner shift $\boldsymbol{\lambda}$ to help the structure in the steady state. Thus the inner shift $\boldsymbol{\lambda}$ between two sub-lattices is absolutely important for deformation gradient of Bravais multi-lattices. It allows the deformation gradient to have self-adjustment so as to reach minimal energy at any time of the deforming process.

6. The hyper-elastic inscribed surface constitutive model for armchair CNTs

The area of representative cell **I** in Fig. 3 is $3\sqrt{3}a_{cc}^{\,2}/4$. In

order to avoid the choice of thickness, the area of surface is adopted to replace the volume of representative cell. The energy associated with a representative cell can be homogenized this energy over its representative inscribed surface Ω_I in the undeformed configuration leads to

$$\bar{W}[\mathbf{F}(\mathbf{X}_\alpha,\boldsymbol{\lambda}),\boldsymbol{\lambda}] = [V(r_{i1}) + V(r_{i2}) + V(r_{i3})]/(2\cdot\Omega_I)\,. \tag{15}$$

By minimizing the strain energy of representative cell with respect to $\boldsymbol{\lambda}$, the inner shift vector can be obtained by

$$\partial\bar{W}[\mathbf{F}(\mathbf{X}_\alpha,\boldsymbol{\lambda}),\boldsymbol{\lambda}]/\partial\boldsymbol{\lambda}\big|_{\boldsymbol{\lambda}=\bar{\boldsymbol{\lambda}}} = 0\,. \tag{16}$$

Then the first Piola-Kirchhoff stress tensor $\bar{\mathbf{P}}$ can be derived by

$$\bar{\mathbf{P}} = \frac{\partial\bar{W}}{\partial\mathbf{F}(\mathbf{X}_\alpha,\boldsymbol{\lambda})}\bigg|_{\boldsymbol{\lambda}=\bar{\boldsymbol{\lambda}}} + \frac{\partial\bar{W}}{\partial\boldsymbol{\lambda}}\frac{\partial\boldsymbol{\lambda}}{\partial\mathbf{F}(\mathbf{X}_\alpha,\boldsymbol{\lambda})}\bigg|_{\boldsymbol{\lambda}=\bar{\boldsymbol{\lambda}}}\,. \tag{17}$$

The modified tangent modulus tensors $\bar{\mathbf{Q}}$ can be expressed as

$$\bar{\mathbf{Q}} = \frac{\partial^2\bar{W}}{\partial\mathbf{F}(\mathbf{X}_\alpha,\boldsymbol{\lambda})^2}\bigg|_{\boldsymbol{\lambda}=\bar{\boldsymbol{\lambda}}} - \left[\frac{\partial^2\bar{W}}{\partial\mathbf{F}(\mathbf{X}_\alpha,\boldsymbol{\lambda})\partial\boldsymbol{\lambda}}\cdot\left(\frac{\partial\bar{W}^2}{\partial\boldsymbol{\lambda}\partial\boldsymbol{\lambda}}\right)^{-1}\cdot\frac{\partial\bar{W}}{\partial\boldsymbol{\lambda}\partial\mathbf{F}(\mathbf{X}_\alpha,\boldsymbol{\lambda})}\right]\bigg|_{\boldsymbol{\lambda}=\bar{\boldsymbol{\lambda}}}\,. \tag{18}$$

Depending on the present model, the energy per atom in both graphite sheet and armchair nanotube can be calculated. Energy per atom in the graphite sheet is -7.3756 eV, which is corresponding to the molecular dynamics simulation of Robertson et al. [6]. For SWCNTs, if the graphite sheet is taken as the ground state, the energy variations from this ground state to the nanotube state can be defined as the strain energy. The strain energy per atom in the armchair CNTs versus the tube's diameter D can be expressed as shown in Fig. 6. This result is in a good agreement with a series of well known simulation results by molecular dynamics [6], tight binding [9] and the exponential Cauchy-Born rule [23].

Based on Cartesian coordinates, Young's modulus of armchair CNTs can be estimated along the axial direction as the following expression:

$$E\cdot h = \bar{\mathbf{Q}}_{1111} - (\bar{\mathbf{Q}}_{1122})^2/\bar{\mathbf{Q}}_{2222}\,, \tag{19}$$

where E is Young's modulus and h is the thickness of carbon nanotubes. If the thickness of a graphite sheet is assumed as 0.335 nm, Young's modulus of graphite sheet by this study is 0.703 TPa, which is in good agreement with that by Zhang et al. [19], the exponential Cauchy-Born rule [23] and the higher order Cauchy-Born rule [24]. Moreover, in order to avoid the choice of tube thickness, the normalized Young's modulus is

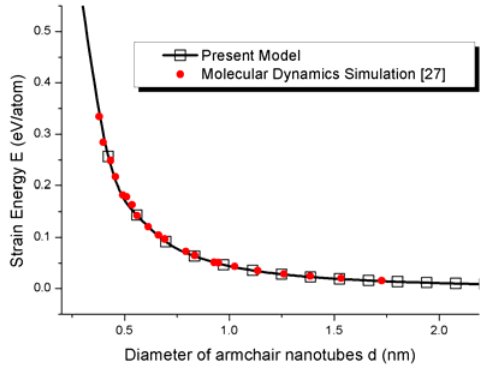

Fig. 6. The strain energy (relative to graphite sheet) per atom in armchair CNTs versus the tube diameter.

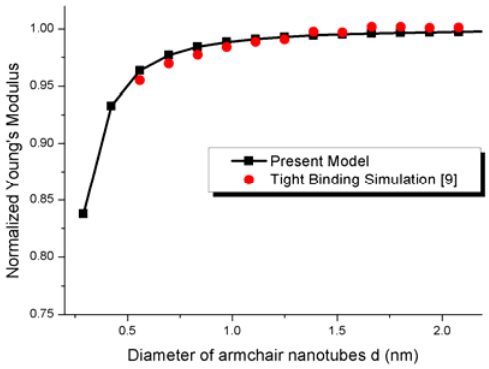

Fig. 7. Young's Modulus of armchair CNTs normalized by that of graphite sheet versus tube diameter.

shown to describe the relationship between graphite sheet and armchair CNTs. The normalized Young's modulus is Young's modulus of nanotube is normalized by that of graphite sheet. The solid line in Fig. 7 shows the normalized Young's modulus versus the nanotube diameter. Based on the same Tersoff-Brenner interatomic potential, the tight-binding simulation results by Goze et al. [9] also are shown by solid circle symbols. It is observed that the results agree well with the tight binding simulation.

Poisson's ratio can be gotten as

$$\nu = \bar{\mathbf{Q}}_{1122}/\bar{\mathbf{Q}}_{1111}\,. \tag{20}$$

The predicted Poisson's ratio of graphite by the present approach is 0.4123, which is the same as the value given by Brenner [27] and the exponential Cauchy-Born rule [23] with using the same interatomic potential. Fig. 8 shows the results versus the tube diameter.

7. Conclusions

A methodology to construct continuum models for armchair CNTs has been developed in the present study. Compared with the atomic surface, it is reasonable and precise to adopt inscribed surface to describe the deformation of CNTs. A

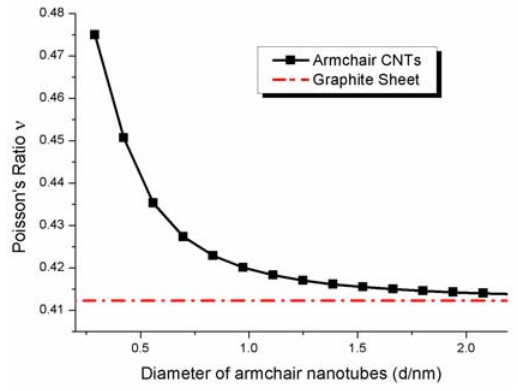

Fig. 8. Poisson's ratio of armchair CNTs versus tube diameter.

hyper-elastic inscribed surface constitutive model by introducing inscribed surface into modified Cauchy-Born rule is proposed. Present study also shows that the inner shift between sub-lattices is absolutely important for deformation of Bravais multi-lattice such as armchair CNTs. It allows the deformation gradient to make self-adjustment so as to reach minimal energy at any time of the deforming process. Resorting to using Tersoff-Brenner potential, the present theory to armchair carbon nanotubes is applied to evaluate the mechanical properties. The results are validated by the comparison with previously reported studies.

Acknowledgment

This work was supported by Inha University, South Korea.

References

[1] S. Iijima, Helical microtubules of graphitic carbon, *Nature(London)* 354 (1991) 56-58.

[2] M. M. J. Treacy, T. W. Ebbesen and J. M. Gibson, Exceptionally high Young's modulus observed for individual carbon nanotubes, *Nature(London)* 381 (1996) 678-680.

[3] A. Krishnan, E. Dujardin, T. W. Ebbesen, P. N. Yianilos and M. M. J. Treacy, Young's modulus of single-walled nanotubes, *Phys. Rev. B* 58 (1998) 14013-14019.

[4] M. F. Yu, O. Lourie, M. J. Dyer, K. Moloni, T. F. Kelly and R. S. Ruoff, Strength and breaking mechanism of multiwalled carbon nanotubes under tensile load, *Science* 287 (2000) 637-640.

[5] M. F. Yu, B. S. Files, S. Arepalli and R. S. Ruoff, Tensile loading of ropes of single wall carbon nanotubes and their mechanical properties, *Phys. Rev. Lett.* 84 (2000) 5552-5555.

[6] D. H. Robertson, D. W. Brenner and J. W. Mintmire, Energetics of nanoscale graphite tubules, *Phys. Rev. B* 45 (1992) 12592-12595.

[7] B. I. Yakobson, C. J. Brabec and J. Bernholc, Nanomechanics of carbon tubes: Instabilities beyond linear response, *Phys. Rev. Lett.* 76 (1996) 2511-2514.

[8] M. Buehler, Mesoscale modeling of mechanics of carbon nanotubes: self-assembly, and fracture, *J. Mater. Res.* 21 (2006) 2855-2869.

[9] C. Goze, L. Vaccarini, L. Henrard, P. Bernier, E. Hernández and A. Rubio, Elastic and mechanical properties of carbon nanotubes, *Synthetic Metals* 103 (1999) 2500-2501.

[10] G. Van Lier, C. Van Alsenoy, V. Van Doren and P. Geerlings, Ab initio study of the elastic properties of single-walled carbon nanotubes and graphene, *Chemical Physics Letter* 326 (2000) 181-185.

[11] G. Zhou, W. H. Duan and B. L. Gu, First-principles study on morphology and mechanical properties of single-walled carbon nanotube, *Chemical Physics Letters* 333 (2001) 344-349.

[12] C. Q. Ru, Axially compressed buckling of a doublewalled carbon nanotube embedded in an elastic medium, *J. Mech. Phys. Solids* 49 (2001) 1265-1279.

[13] J. Z. Liu, Q. Zheng and Q. Jiang, Effect of a rippling mode on resonances of carbon nanotubes, *Phys. Rev. Lett.* 86 (2001) 4843-4846.

[14] C. Y. Li and T. W. Chou, A structural mechanics approach for analysis of carbon nanotubes, *International Journal of Solids and Structures* 40 (2003) 2487-2499.

[15] E. B. Tadmor, M. Ortiz and R. Phillips, Quasicontinuum analysis of defects in solids, *Philos. Mag. A* 73 (1996) 1529-1563.

[16] E. B. Tadmor, R. Phillips and M. Ortiz, Mixed atomistic and continuum models of deformation in solids, *Langmuir* 12 (1996) 4529-4534.

[17] H. Gao, Y. Huang and F. A. Abharam, Continuum and studies of intersonic crack propagation, *J. Mech. Phys. Solids* 49 (2001) 2113-2132.

[18] P. Zhang, Y. Huang, H. Gao and K. C. Hwang, Fracture nucleation in single-wall carbon nanotubes under tension: a continuum analysis incorporating interatomic potentials, *J. Appl. Mech.* 69 (2002) 454-458.

[19] P. Zhang, Y. Huang, P. H. Geubelle, P. A. Klein and K. C. Hwang, The elastic modulus of single-walled carbon nanotubes: a continuum analysis incorporating interatomic potentials, *Int. J. Solids Struct.* 39 (2002) 3893-3906.

[20] P. Zhang, H. Jiang, Y. Huang, P. H. Geubelle and K. C. Hwang, An atomistic-based continuum theory for carbon nanotubes: analysis of fracture nucleation, *J. Mech. Phys. Solids* 52 (2004) 977-998.

[21] H. Jiang, P. Zhang, B. Liu, B., Y. Huang, P. H. Geubelle, H. Gao and K. C. Hwang, The effect of nanotube radius on the constitutive model for carbon nanotubes, *Comput. Mater. Sci.* 28 (2003) 429-442.

[22] M. Arroyo and T. Belytschko, An atomistic-based finite deformation membrane for single layer crystalline films, *J. Mech. Phys. Solids* 50 (2002) 1941-1977.

[23] M. Arroyo and T. Belytschko, Finite crystal elasticity of carbon nanotubes based on the exponential Cauchy–Born rule, *Phys. Rev. B* 69 (2004) 115415 1-11.

[24] X. Guo, J. B. Wang and H. W. Zhang, Mechanical properties of single-walled carbon nanotubes based on higher order

Cauchy-Born rule, *Int. J. Solids Struct.* 43 (2006) 1276-1290.
[25] S. Lu, C. D. Cho and L. Song, Energy of armchair nanotube using the modified Cauchy-Born rule, *Int. J. Mod. Phys. B* 22 (31-32) (2008) 31-32 5881-5886.
[26] J. Tersoff, New empirical approach for the structure and energy of covalent systems, *Phys. Rev. B* 37 (1988) 6991-7000.
[27] D. W. Brenner, Empirical potential for hydrocarbons for use in simulation the chemical vapor deposition of diamond films, *Phys. Rev. B* 42 (1990) 9458-9471.
[28] M. Born and K. Huang, *Dynamical Theory of Crystal Lattice*, Oxford University Press, Oxford, USA (1998).
[29] E. B. Tadmor, G. S. Smith, N. Bernstein and E. Kaxiras, Mixed finite element and atomistic formulation for complex crystals, *Phys. Rev. B* 59 (1999) 235-245.
[30] Y. L. Mao, X. H. Yan, Y. Xiao, J. Xiang, Y. R. Yang and H. L. The viability of 0.3 nm diameter carbon nanotubes, *Nanotechnology* 15 (2004) 1000-1003.

Sheng Lu received his B.S. degree in Engineering Mechanics from Xi`an Jiaotong University of China in 2004 and his Ph.D. degree in Mechanical Engineering from Inha University of S. Korea in 2009. His interests include atomistic-continuum theory, mechanics of composite materials, structural analysis.

Chongdu Cho received the B.S. degree in mechanical engineering from Seoul National University of Korea in 1983. He received the M.S. degree in mechanical engineering from Korea Advanced Institute of Science and Technology in 1985 and Ph.D. degree in mechanical engineering and applied mechanics from Michigan University of USA in 1991. His research interests include thermal stress analysis, structural analysis, mechanics of composite materials, MEMS, biomechanics, and nano mechanics.